

# Image segmentation using multi-coloured active illumination

Tze Ki Koh<sup>1,2</sup>, Nicholas Miles<sup>1</sup>, Steve Morgan<sup>2</sup>, Barrie Hayes-Gill<sup>2</sup>

<sup>1</sup>School of Chemical, Environmental and Mining Engineering, <sup>2</sup>School of Electrical and Electronic Engineering  
University of Nottingham, University Park, Nottingham NG7 2RD, United Kingdom

Email: {enxtkk, nick.miles, steve.morgan, barrie.hayes-gill}@nottingham.ac.uk

**Abstract**— In this paper, the use of active illumination is extended to image segmentation, specifically in the case of overlapping particles. This work is based on Multi-Flash Imaging (MFI), originally developed by Mitsubishi Electric Labs, to detect depth discontinuities. Illuminations of different wavelengths are projected from multiple positions, providing additional information about a scene compared to conventional segmentation techniques. Shadows are used to identify true object edges. The identification of non-occluded particles is made possible by exploiting the fact that shadows are cast on underlying particles. Implementation issues such as selecting the appropriate colour model and number of illuminations are discussed. Image segmentation using the proposed method, canny edge detection and watershed transform are performed on overlapping beach pebbles and granite. Evaluation results confirm that the proposed method is a successful extension of the original method and reveals its increased accuracy when compared with conventional segmentation techniques.

**Index Terms**—multi-flash, image segmentation, active illumination, shadows, particle size analysis

## I. INTRODUCTION

An accurate calculation of the size distribution of particles is crucial in the mining and quarrying industry. It is used to assess the quality of particulate material after or prior to operations such as crushing or blasting. Sieving is a traditional method where particles are passed through grids of variable mesh sizes to determine their size distribution based on their diameter. These systems require representative samples to be taken, with the inherent errors that this can involve. Offline analysis also means that the data collected is out of date. This has a significant impact where out of specification or contaminating materials are loaded into the wrong bunkers for example. Therefore, online systems are often used as they have obvious advantages over traditional mechanical sieving methods which are labour and time intensive.

Machine vision in automated particle size analysis has been an active research area for many years [1]-[5]. Accurate calculations are strongly dependent on the efficiency of the image processing steps, particularly image segmentation. Even if a proficient mathematical model was used to produce a size distribution of an image

with poorly segmented particles, the results would be inaccurate due to the poor quality input data.

Image segmentation is an intrinsic determinist in the performance of computer vision applications as it directly influences the efficiency of subsequent image processing steps. Accurate identification of the region(s) of interest in an image is critical if one were to perform image analysis successfully. Numerous approaches and techniques have been developed to meet this need over the past few decades [6]-[8]. However, due to the diversity and complexity of scenes, there is no single technique which produces the best result for every application [9].

It is difficult for segmentation algorithms to distinguish between overlapping particles with a similar texture and colour due to poor contrast between their edges. Moreover, overlapping particles cause errors in size measurements as partially visible particles are taken to be representative of entire particles.

Wang and Stephansson [5] developed image processing algorithms aimed at enhancing the contrast between touching particles, removing bright spots and smoothing greyscale variations. This included methods to merge and split regions based on their common boundary and arc lengths. Maerz [2] employed thresholding, gradient operators and reconstruction techniques to segment particles in the image.

No significant attention has been given to the illumination of the images prior to segmentation. The purpose of illumination has been purely to provide sufficient light to capture a clear image of the particle. Illumination, however, plays a key role in the quality of images which can be exploited further to enhance the performance of image segmentation. Different illumination configurations provide additional information about a scene.

This paper extends the use of an active illumination approach to image segmentation based on Multi Flash Imaging (MFI) developed by Mitsubishi Electric Research Labs [10]. Raskar and his team made use of strategically positioned flashes to produce an edge depth map computed from a series of images. In this paper, multi-coloured lamps are used in place of the flashes which allows simultaneous acquisition of the images. A novel method of discriminating between non-occluded particles and underlying particles is also demonstrated.

This is relevant to a wide range of scenes containing overlapping particles, extending from analysing grains in the food industry [11] [12] to rocks in the mining industry [13].

Section II provides a description of the proposed method and Section III covers the implementation aspects. Section IV shows evaluation results while conclusion and future work are discussed in Section V.

## II. MULTI-COLOURED ACTIVE ILLUMINATION

### A. Use of uniquely coloured illuminations

Multi-flash imaging was originally performed using images captured sequentially, with a time lapse between them. Scenes were illuminated with the same colour but from different directions, one after another. The different instances in time where each image was taken meant that in a dynamic scene, the images change. This poses a problem in situations such as a moving conveyor belt where the scene contains moving particles. Thus, shadows cast from the same particle in a later image would not be from its former position in an earlier image.

The proposed method utilises multi-coloured illuminations which addresses the problem of a dynamic scene. Instead of triggering each illumination in a timely fashion, uniquely coloured illuminations project shadows in different directions simultaneously. This allows the capture of a single image which preserves the spatial information of the particles through the analysis of its respective colour planes. The proposed method can be employed without interrupting the operations of the conveyor belt. The operating speed at which the proposed method can run smoothly depends on the intensity of the illumination and shutter speed of the image capture device.

### B. Algorithm

The algorithm is described using 3 colours as this is compatible with standard RGB cameras, although it can be extended to  $n$  colours with the use of appropriate multi-spectral cameras. The steps involved in the algorithm are shown in Fig 1.

#### Step 1: Single image capture with multiple illuminations

The scene is illuminated by 3 different coloured illuminations, each 120 degrees apart. A single static image,  $I(x)$ , is taken of the scene where shadows of different colours are cast around the object(s) of interest.

#### Step 2: Separation into RGB planes

$I(x)$  is separated into its red, green and blue colour planes, namely  $I_{red}(x)$ ,  $I_{green}(x)$  and  $I_{blue}(x)$  respectively. Red coloured light illuminates the object from the bottom right corner, causing a shadow in the top left corner. As this shadow is caused by the absence of red illumination, it can be identified as dark regions in  $I_{red}(x)$  as shown in Fig 1. Similarly, shadows caused by the green and blue illuminations can be detected in their respective colour planes. This allows the detection of shadows cast on

different sides of the object concurrently in a single image.

#### Step 3: Finding the max intensity image

Fig 1 shows the maximum intensity image computed by

$$I_{max}(x) = \max(I_{red}(x), I_{green}(x), I_{blue}(x)) \quad (1)$$

where  $I_{max}(x)$  contains the highest intensity value of every pixel amongst the colour planes. The intention of this step is to eliminate all regions where shadows exist. In the case where the multiple light sources are of uniform intensity and distributed evenly around and close to the camera's centre of projection (COP), we can assume that  $I_{max}(x)$  is a close estimation of having an image taken with a single white light source at the camera's COP.

#### Step 4: Find ratio images

The ratio images are computed by dividing each plane image by the maximum intensity image:

$$R_C(x) = \frac{I_C(x)}{I_{max}(x)} \quad \text{for } C = red, green, blue \quad (2)$$

Each pixel in the ratio image,  $R_C(x)$  has a value of zero in shadowed regions and tends to unity in illuminated regions. The ratio image accentuates the shadows and suppresses the texture.

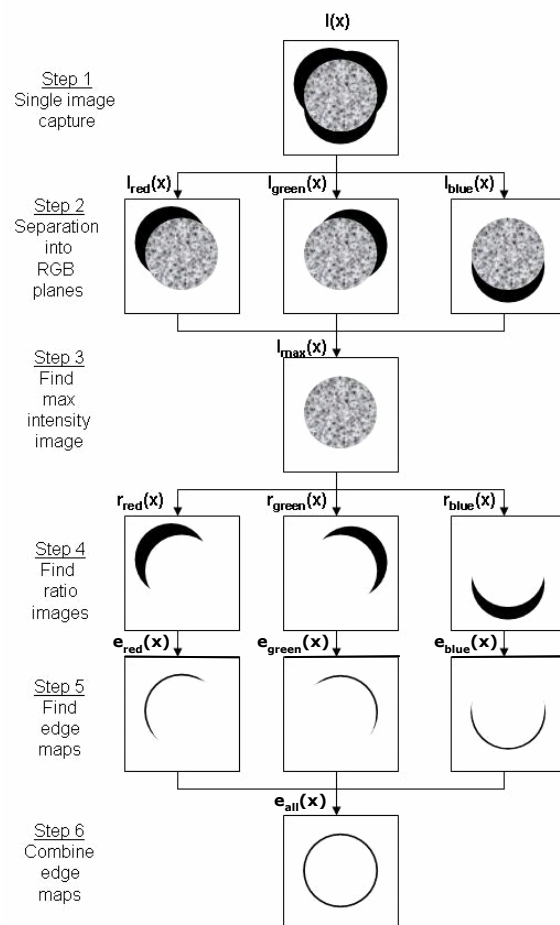


Figure 1. Steps involved in the proposed method.

Step 5: Find edge maps

The edge maps can be found by convoluting the ratio images with different masks and applying a threshold.

$$e_{red}(x) = \left( r_{red}(x) * \begin{pmatrix} -1.4 & -1.4 & 0 \\ -1.4 & 0 & 1.4 \\ 0 & 1.4 & 1.4 \end{pmatrix} \right) > thres \quad (3)$$

$$e_{green}(x) = \left( r_{green}(x) * \begin{pmatrix} 0 & -1.4 & -1.4 \\ 1.4 & 0 & -1.4 \\ 1.4 & 1.4 & 0 \end{pmatrix} \right) > thres \quad (4)$$

$$e_{blue}(x) = \left( r_{blue}(x) * \begin{pmatrix} 1 & 2 & 1 \\ 0 & 0 & 0 \\ -1 & -2 & -1 \end{pmatrix} \right) > thres \quad (5)$$

Applying an edge detector such as the Sobel operator on the ratio images produces an intensity gradient image. At an object's edge where a shadow starts, there would be a significant intensity change along the epi-polar ray originating from the light source. Only pixels with intensity transitions from illuminated to shadowed regions are detected by specifying the gradient direction in the filter. This eliminates false edges between the shadows and the background. In addition, only pixels with intensity transitions beyond a certain threshold are considered as an edge. A two level edge threshold is employed for this purpose. Edges present in the low level confidence map would only be considered as true edges if they are 8-connected to edges in the high level confidence map. Thresholds are determined manually.

Step 6: Combine edge maps

$$e_{all}(x) = e_{red}(x) | e_{green}(x) | e_{blue}(x) \quad (6)$$

The three edge maps are combined using the OR operation to form a final edge map showing edges in all directions. In a real application, the final edge map often contains missing edges along true boundaries and false edges within the object itself.

C. Identification of non-occluded particles

Due to the inherent limitation of 2D imaging in the visible spectrum, the image capture device is able to obtain a view only from the top of the scene as shown in Fig 2(a). Underlying particles which are partially visible from the top would undeniably cause measurement errors if their partial visible surface area were taken to be representative of the entire particle.

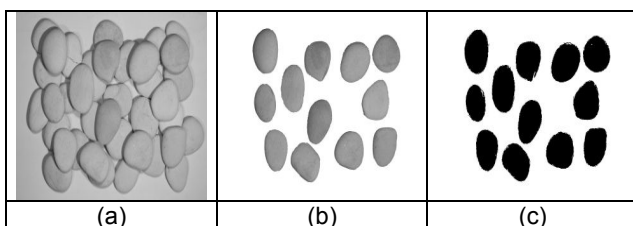


Figure 2. (a) Top view of overlapping particles (b) Manual identification of non-occluded particles (c) Automatic identification of non-occluded particles

Thurley and Ng [14] address this problem through the use of three dimensional imaging. A surface topology of the scene is expressed in terms of three dimensional data through the use of a custom built active triangulation system utilising a single CCD camera and projector. Non-occluded particles can be identified by exploiting the additional depth dimension otherwise absent in two dimensional images. Thurley and Ng [14] reaffirms that ‘Such a capability provides a significant advantage in the classification of fragments over photographic-based methods as it eliminates bias due to the treatment of partially visible fragments as if they were smaller entirely visible fragments.’

While MFI is not an entirely three dimensional technique, it does provide extra information beyond two dimensional techniques. The use of shadows can be used to infer information about the placement of objects in a scene, for example, identification of non-underlying particles. Quite simply, underlying particles will have shadows cast upon them by the particles near to the top of the pile. Particles that have a significant proportion of their area in shadow can be identified as an underlying particle.

This is achieved through the use of a shadow map which contains pixels below a threshold amongst all of the ratio images, revealing shadows from all three illumination sources. This allows measurement of the amount of shadow which falls on each region in the edge map. A region with shadows above a defined threshold is likely to be part of a particle which is partially covered by other particles. This provides an extremely convenient and simple solution compared to conventional three dimensional imaging in the identification of non-occluded particles.

Fig 2 shows how MFI can be extended to identify non-occluded particles automatically. Non-occluded particles were identified both manually using Photoshop and automatically using MFI. All the non-occluded particles were identified, as shown in Fig 2(c).

III. IMPLEMENTATION

A. Number of illuminations

It is essential for each illumination to be of a unique colour. The number of illuminations determines the number of non-overlapping bands in which the image has to be analysed. Intuitively, a larger number of illuminations evenly distributed around the object would allow coverage of a wider range of angles in which edges may be detected. This however, increases complexity, cost and may reduce intensity levels due to narrower spectral filtering. Three illuminations have been used in this paper as it has been found to be an ideal balance in the trade-off between performance and ease of implementation. Fig 3 shows the shadows around a glass sphere of 20mm in diameter being illuminated by three unique colours. Shadows have been cast around the entire particle by at least one of the illuminations. Furthermore, there are certain overlapping shadows which are caused by two illumination sources. The three illuminations are

120 degrees apart and on the same plane as the image sensor.

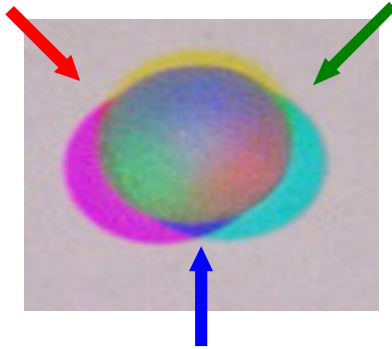


Figure 3. Sphere illuminated with 3 colours

### B. Selection of colour model

Colour can be represented by different models, each with its unique strengths and suitable applications. Some examples include RGB, normalised RGB, HSI and CIE [8].

RGB is the most widely used model for displaying images on a monitor and storing images taken by digital cameras. Let R, G and B represent the tri-stimulus components obtained from a colour camera to define images taken from the sensor space:

$$C = \int_{\lambda} E(\lambda)U_C(\lambda)d\lambda \text{ for } C \in (R, G, B) \quad (7)$$

where  $E(\lambda)$  is the radiance spectrum and  $U_C$  are the three colour filter transmission functions.

Sensors often do not receive uniform radiance across the whole sensor space due to non-uniform lightning intensities. The normalised RGB (Nrgb) model corrects for this by normalising the intensities across the spectral distribution.

This prevents colour fluctuations due to uneven lighting and is derived from the RGB model as follows:

$$r = \frac{R}{(R + G + B)} \quad (8)$$

$$g = \frac{G}{(R + G + B)} \quad (9)$$

$$b = \frac{B}{(R + G + B)} \quad (10)$$

The HSI model breaks down an image into its hue, saturation and intensity planes. It can be derived from either the RGB or Nrgb model. Hue represents the actual colour and is determined by the dominant wavelength of light received. Saturation reveals the purity of the colour, which reveals the degree of whiteness mixed with the hue. Colour information is solely defined by hue and saturation values while intensity provides a measure of the image's brightness, determined by the amount of light received.

Fig 4 shows the edge map of the sphere shown in Fig 3 computed by the proposed method using the Nrgb and



Figure 4. (a) Edge map produced using Nrgb model (b) Edge map produced using HSI model

HSI models. The HSI model failed to detect parts of the boundary where shadows are caused by two overlapping illumination sources. The HSI model provides greater discrimination between colours and therefore fails to detect overlapping shadows of different colours. On the other hand, there is high correlation between the r, g and b components of the Nrgb model. This allows overlapping shadows to be detected in edge maps from two illumination sources instead of one, thus increasing the accuracy of segmentation. The Nrgb model is used in the proposed method as it also provides normalisation of any intensity variations across the colour planes.

### C. Hardware setup

A Nikon D100 digital SLR camera was used as the image capture device. 500W spotlights were used as light sources, contained in a pyramid shaped holder as shown in Fig 5. Colour filters (Lee, USA) were placed at the base of the holders to provide different coloured illuminations. This eliminates the need for individual triggering of each illumination. Furthermore, as spotlights are used instead of flashes, they can be operated continuously and the only device which needs to be controlled is the SLR camera. The SLR camera is connected to a desktop computer which runs Nikon capture software to automate the capture and storage of images. Matlab was used to perform all image processing algorithms.

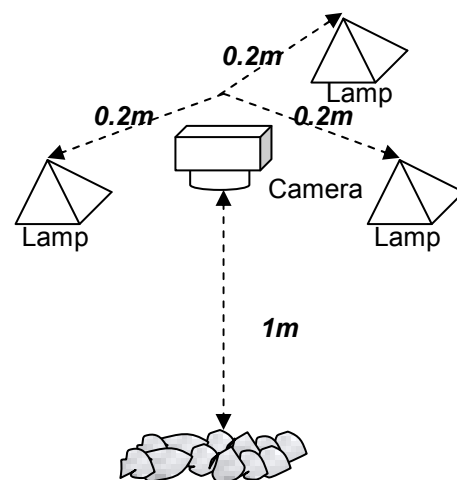


Figure 5. Hardware setup of camera with different illuminations

IV. EVALUATION

In order to evaluate its performance in image segmentation, our proposed method was compared with two commonly used segmentation techniques, namely watershed transform and canny edge detection applied to the conventional (white light) image. Marker controlled watershed transform was used to reduce the problem of over-segmentation through automatic seed selection by morphological operations [15]. The canny edge detection was applied with thresholds determined manually.

The proposed method was evaluated on two types of particles, namely beach pebbles and limestone, each with different geometric properties. Shown in Fig 6 are results from the beach pebbles over a field of view of 150x150mm. The proposed method produced clean and comparatively accurate boundaries (Fig 6(ii)). All of the non-occluded pebbles identified manually in Fig 6(iii) were detected by the proposed method (Fig 6(iv)). A few particles which were slightly occluded were also detected because they were below the shadow threshold. Whilst the watershed transform (Fig 6(v)) produced enclosed regions without any boundary gaps, there were errors in the edge map and there is no way of identifying non-occluded particles. This is true also for the canny edge detection (Fig 6(vi)), which failed to differentiate between regions of low contrast.

Fig 7 shows the results from a pile of limestone. The edges detected by the proposed method contain more errors due to shadows caused by the angular surfaces compared to the beach pebbles. The inaccuracies in the edge map led to errors in the identification of non-occluded particles shown in Fig 7(iv). Some regions belonging to different particles were combined and regions belonging to occluded particles were wrongly identified. However, the proposed method produced more visually accurate results as compared to the watershed transform and canny edge detection (Figs 7(v) and 7(vi) respectively).

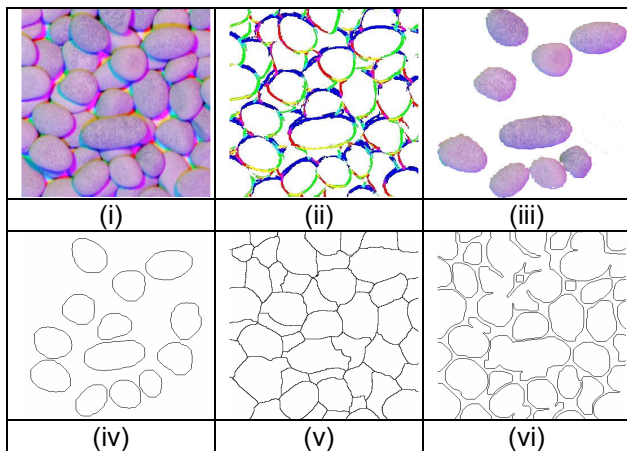


Figure 6. (i) Beach pebbles illuminated with RGB lights (ii) Edge map computed using multi-colour active illumination (iii) Manual identification of non-occluded particles using Photoshop (iv) Automatic identification of non-occluded particles (v) Edge map computed using marker-controlled watershed transform (vi) Edge map computed using canny edge detection

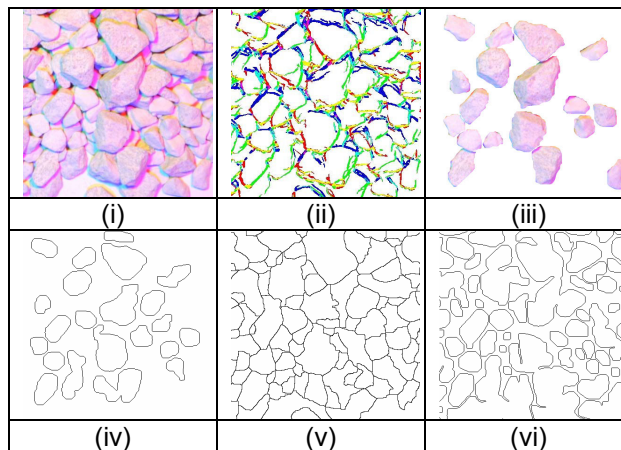


Figure 7. (i) Limestone illuminated with RGB lights (ii) Edge map computed using multi-colour active illumination (iii) Manual identification of non-occluded particles using Photoshop (iv) Automatic identification of non-occluded particles (v) Edge map computed using marker-controlled watershed transform (vi) Edge map computed using canny edge detection

From the results shown, the proposed method produced less irrelevant regions (such as underlying particles) as compared to the other techniques. While the watershed technique is able to produce complete boundaries, it faces the problem of over-segmentation. Furthermore, it has the tendency to enlarge regions beyond the surface area of the particles. The canny edge detector failed to identify several substantial edges between particles. While our proposed method is also subject to missing edges, they are fewer and more likely belong to occluded particles. Both the watershed transform and canny edge detection have no way of ensuring that regions belong to unoccluded particles.

V. FUTURE WORK AND CONCLUSION

A. Future work

In real world scenarios, conveyor belts are moving. This was the underlying impetus for our proposed method which uses a single image. Further investigations will evaluate our proposed method on a moving conveyor belt with varying speeds.

It has been demonstrated that the geometric properties of the particles affect the performance of our proposed method. Ideal particles should have a similar and smooth texture which reduces the detection of surplus edges within the particle surfaces. Furthermore, our proposed method is dependent on the albedo of the particles. Problems may arise if some particles in the same scene are more reflective in the bandwidth of one of the illuminations. There is therefore a need for further investigation of the performance of our proposed method on a wider range of particles and numerical results to provide quantitative evaluation of the performance.

B. Conclusion

The extension of the original MFI technique using RGB planes has proved to be successful and have been applied to the image segmentation of particles. Results reveal the potential of the proposed method when

compared with conventional segmentation techniques. Overlapping particles can result in incorrect measurement of particle size, and this is dealt with in our proposed method. This is accomplished without the complexities of 3D imaging, but rather, with different coloured illuminations which can be implemented easily. Our proposed method brings us a step closer to the realisation of a system operating on a dynamic conveyor belt.

#### ACKNOWLEDGEMENT

The authors wish to thank Dr Ramesh Raskar and Dr Amit Agrawal from Mitsubishi Electric Research Labs (MERL) for their support and technical advice. Tze Ki Koh is funded by a studentship from the University of Nottingham.

#### REFERENCES

- [1] C. L. Lin, Y. K. Yen and J. D. Miller, "Plant-site evaluations of the OPSA system for on-line particle size measurement from moving belt conveyors," *Minerals Engineering*, vol. 13, pp. 897-909, 2000.
- [2] N. H. Maerz, "Aggregate sizing and shape determination using digital image processing," *Center for Aggregate Research (ICAR) Sixth Annual Symposium Proceedings*, pp. 195-203, 1998.
- [3] S. G. Mkwelo, F. Nicolls and G. De Jager, "Watershed-based segmentation of rock scenes and proximity-based classification of watershed regions under uncontrolled lighting conditions," *Proceedings of 14th Annual Symposium of the Pattern Recognition Association of South Africa (PRASA)*, pp. 107-112, 2003.
- [4] R. A. Salinas, U. Raff and C. Farfan, "Automated estimation of rock fragment distributions using computer vision and its application in mining," *IEE Proceedings-Vision, Image, and Signal Processing*, vol. 152, pp. 1-8, 2005.
- [5] W. X. Wang and O. Stephansson, "On-line system for monitoring the size distribution of aggregates on a conveyor belt," *Measurement of Blast fragmentation*, pp. 167-174, 1996.
- [6] K. S. Fu and J. K. Mui, "A survey on image segmentation," *Pattern Recognition*, vol. 13, pp. 3-16, 1981.
- [7] N. R. Pal and S. K. Pal, "A review on image segmentation technique," *Pattern Recognition*, vol. 26, pp. 1277-1294, 1993.
- [8] H. D. Cheng, X. H. Jiang, Y. Sun and J. Wang, "Color image segmentation: advances and prospects," *Pattern Recognition* 34, vol. 12, pp. 2259-2281, 2001.
- [9] T. Zouagui, H. Benoit-Cattin and C. Odet, "Image segmentation functional model," *Pattern Recognition*, vol. 37, pp. 1785-1795, 2004.
- [10] R. Raskar, K. H. Tan, R. Feris, J. Yu and M. Turk, "Non-photorealistic camera: depth edge detection and stylized rendering using multi-flash imaging," *ACM Transactions on Graphics (TOG)*, vol. 23, pp. 679-688, 2004.
- [11] B. Tadhg and W. S. Da, "Inspection and grading of agricultural and food products by computer vision systems—a review," *Computers and Electronics in Agriculture*, vol. 36, pp. 193-213, 2002.
- [12] J. D. Cheng and W. S. Da, "Recent developments in the applications of image processing techniques for food quality evaluation," *Trends in Food Science & Technology*, vol. 15, pp. 230-249, 2004.
- [13] E. Cabello, M. A. Sanchez and J. Delgado, "A New Approach to Identify Big Rocks with Applications to the Mining Industry," *Real-Time Imaging*, vol. 8, pp. 1-9, 2002.
- [14] M. J. Thurley and K. C. Ng, "Identifying, visualizing, and comparing regions in irregularly spaced 3D surface data," *Computer Vision and Image Understanding*, vol. 98, pp. 239-270, 2005.
- [15] R. C. Gonzalez, R. E. Woods and S. L. Eddins, *Digital Image Processing Using Matlab*. Prentice Hall, 2004.

**Tze Ki Koh** is a PhD student at the University of Nottingham, investigating novel computer vision methods of particle sizing and segmentation of aggregates on conveyor belts. He is jointly funded by the University of Nottingham International Office, School of Chemical, Environmental and Mining Engineering and the School of Electrical and Electronic Engineering.

**Professor Nick Miles** is the Head of the School of Chemical, Environmental and Mining Engineering at the University of Nottingham, is a mineral processing engineer with over 20 years international experience in teaching, research and consultancy. He has extensive knowledge of, and research experience in fine particle processing, waste minimisation and recycling, bulk material transportation processes and coal preparation. Professor Miles has a research philosophy with collaboration at its core - working in interdisciplinary teams exploring fundamental scientific issues through to the exploitation and commercialisation of research.

**Dr Steve Morgan** is an Associate Professor and Reader in Biomedical Optics at the University of Nottingham. Since 1992 he has been researching novel optical techniques for imaging and spectroscopy of tissue. In 1998 he was awarded an Engineering and Physical Sciences Research Council (UK) Advanced Fellowship to perform research in biomedical optics. His research involves the development of novel optical devices to monitor the skin for applications such as skin cancer diagnosis and blood flow measurement. Recently, he has been investigating novel methods of sensing and imaging in machine vision applications.

**Dr Barrie Hayes-Gill** is an Associate Professor within the School of Electrical and Electronic Engineering. He has over 25 years experience working in the area of environmental and physiological electronic instrumentation having collaborated with clinical colleagues and industry on numerous projects. These include the application of electronic and optical techniques to health monitoring and the telemetry and processing of environmental and physiological signals. Dr Hayes-Gill has published over 150 papers, holds five patents and is an author of an undergraduate textbook and to date. Dr Hayes-Gill is a Chartered Engineer and a Eur Ing and is a member of both the Institute of Electrical and Electronic Engineers (IEEE) and the Institute of Electrical Engineers (IEE).